[9]The ambiguity of this type in the light-cone expansion is discussed in some detail by Wilson. See K. Wilson, in *Proceedings of the International Symposium on Electron and Photon Interactions at High Energies*, edited by N. B. Mistry (Cornell Univ. Press, Ithaca, N. Y., 1972), p. 115. Application of the Wilson expansion to $J_\mu(x)J_\nu(0)$ at $x \sim 0$ shows that the right-hand side of (17) contains a term

$$\sim \lim_{s\to\infty} \lim_{x\to 0} (sx^2)^{-1} \times C_{\pi\sigma} \langle p_1, p_2 | \theta^{\pi\sigma}(0) | p_1, p_2 \rangle$$

($C_{\pi\sigma}$ is a constant and $\theta^{\pi\sigma}$ is the stress-energy tensor), which clearly exhibits the ambiguity involved in the sum rule (17).

PHYSICAL REVIEW D VOLUME 8, NUMBER 9 1 NOVEMBER 1973

Resonance and Parton-Model Descriptions of Final States of Deeply Inelastic Reactions

J. Kogut*
Institute for Advanced Study, Princeton, New Jersey 08540
(Received 9 April 1973)

It is pointed out within the context of parton and resonance models that identical physics governs the threshold regions of seemingly distinct inclusive spectra. For example, the threshold region of νW_2 and the edge of the current fragmentation region of deeply inelastic reactions share identical descriptions. This idea is made explicit within the context of an intuitive quark-parton model in which only ordinary hadrons are produced as the result of deeply inelastic collisions. The properties of the distribution in momentum space of these hadrons are discussed and a realization of Bjorken's correspondence method is obtained. Relations between the shape of the hadron spectrum near the edge of the current fragmentation region, Regge intercepts, and the asymptotic falloff of elastic and transition form factors emerge.

I. INTRODUCTION

A challenging problem for both theoretical and experimental high-energy physicists is the study of the final hadronic states produced in deeply inelastic reactions [$e^+e^- \to$ virtual photon $\to$ hadron +anything, e (ν) +hadron $\to e$ (μ) +hadron′ +anything, etc.]. Since a study of electroproduction (e +hadron $\to e$ +anything) has revealed a number of profound features of hadrons,[1] we can anticipate that the study of final states will be equally spectacular.

Of particular interest is the character of the secondary hadrons which in the lab frame carry a finite fraction of the photon's energy. It is the purpose of this short article to propose a description of the distribution of these hadrons—the fragments of the virtual photon. In this attempt we are motivated by (1) the Bloom-Gilman[2] analysis of νW_2, and (2) the quark-parton model. It is suggested that the resonant character of hadronic matter is an essential feature of an understanding of the final hadronic states produced in deeply inelastic reactions. This idea sheds some light on the the intuitive quark-parton picture of final states. Our approach is illustrated in an application to determine the shape of the inclusive hadron spectrum in the virtual-photon fragmentation region. Relations between the shape of the spectrum near the kinematic boundary, Regge intercepts, and the asymptotic falloff of elastic and transition form factors emerge. These arguments provide a realization of Bjorken's correspondence method.[3,4]

This article is organized as follows: In Sec II we review both the resonance model and the quark-parton model approaches to the threshold behavior of νW_2. Then exclusive electroproduction at high $\omega'(=1+s/Q^2)$ is discussed in Sec. III and the lessons learned in Sec. II are applied here. It is argued that identical dynamical mechanisms govern both regions. Summing over exclusive electroproduction channels yields a scaling result for σ_{tot}. Quarks do not appear in the final state. The character of the hadron distribution in the virtual-photon fragmentation region is discussed in Sec. IV. Within the context of a world of hadron resonances, it is argued that this distribution may be similar to that encountered in ordinary hadronic reactions. A comparison is made with the intuitive quark-parton picture of final states. In Sec. V an inclusive-exclusive argument is presented within the proposed framework. Connections obtained elsewhere by more general correspondence arguments emerge. General discussion and comments

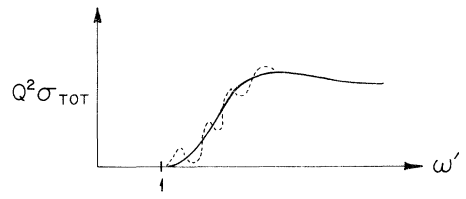

FIG. 1. The structure function νW_2 plotted against ω'. The dashed curve depicts the contribution for discrete resonances at finite Q^2. The smooth curve is the asymptotic ($Q^2 \to \infty$) scaling curve—it averages the dashed curve.

appear in Sec. VI. These include remarks on particle ratios in the photon-fragmentation region, and the compatibility of this approach with the light cone.

II. TWO DESCRIPTIONS OF νW_2

A. Resonance Models

Our method of attack is inspired by the Bloom-Gilman[2] analysis of νW_2, so we review that briefly.[5] Consider the scaling variable $\omega' = 1 + s/Q^2$. The electroproduction of particular nucleon resonances (of mass M_m) then appear as resonance bumps at $\omega'_m = 1 + M_m^2/Q^2$ in the total electroproduction cross section (Fig. 1). As $Q^2 \to \infty$, the recognizable resonances are pushed towards $\omega' = 1$, but it has been suggested (with considerable experimental support[6]) that the area under a resonance bump (Fig. 1) remains a finite fraction of the scaling function $\nu W_2(\omega')$ at the corresponding ω'. This requires, as first noticed by M. Elitzur,[7] that the nucleon-transition form factors be given by a universal function of Q^2/M_m^2. One is then led to consider a resonance dominance expression for νW_2,

$$\nu W_2 = 2\nu \sum_m G^2\left(\frac{Q^2}{M_m^2}\right)\delta(s - M_m^2), \tag{1}$$

where G is the universal nucleon-transition form factor. For large s one expects many resonances to contribute, so it is sensible to approximate Eq. (1) with an integral,

$$\begin{aligned} \nu W_2 &= \omega Q^2 \int G^2\left(\frac{Q^2}{M^2}\right)\rho(M^2)\delta(s - M^2)\,dM^2, \\ \nu W_2 &= \omega Q^2 \rho(s) G^2((\omega' - 1)^{-1}), \end{aligned} \tag{2}$$

where $\rho(s)$ is the density of resonances of mass $\sqrt{s}$ coupling to the virtual photon. Requiring that Eq. (2) scale implies that $\rho(s) \sim s^{-1}$.[8] Then,

$$\nu W_2 = \frac{\omega}{\omega' - 1} G^2((\omega' - 1)^{-1}). \tag{3}$$

If G is power-behaved for large values of its argument, $G(y) \sim y^{-n}$, say, then Eq. (3) implies that νW_2 has the threshold behavior

$$\nu W_2 \sim \omega(\omega' - 1)^{2n-1}. \tag{4}$$

This relationship between the rate of decrease of form factors and the threshold behavior of νW_2 agrees with that originally found by Drell and Yan,[9] and West[10] in composite models.

This presentation of the s-channel resonance approach to νW_2 is much cruder than it need be. For example, for each mass M_m one expects a large number of resonances, each labeled, in addition, by its spin, parity, etc. Also, high-mass resonances are expected to be very unstable, so one should at least equip Eq. (1) with resonance widths. These modifications of the naive discussion given here have been carried out within particular models.[11] The same rough connections as made here survive a more realistic presentation.

B. Parton Model

A similar description of the threshold behavior of νW_2 also emerges from the parton model.[12] Since closely related ideas will play a role in later discussions, this problem will be discussed in some detail. Consider a hadron moving in the $+z$ direction with very large momentum P. In such a frame one can consider the parton distribution within the hadron. As shown in Fig. 2(a), the most likely parton distribution on the rapidity axis is roughly flat and extends from rapidity $y \approx \ln(2P/m)$ to $y \approx 0$.[13] In a deep-inelastic collision a photon with zero energy and momentum $q_z = -2xP$ is absorbed by a parton with momentum $p_z = xP$. The parton's final momentum is $p'_z = -xP$ ($x = -q^2/2q \cdot p$ is Bjorken's scaling variable.)[14] So, immediately after the collision the parton configuration is that in Fig. 2(b). If x is very close to

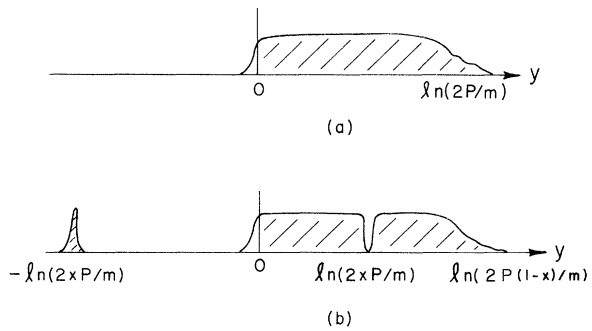

FIG. 2. (a) The distribution of partons in a hadron having rapidity $\ln(2P/m)$. (b) The parton distribution immediately after the absorption of a virtual photon. Note the hole at rapidity $\ln(2xP/m)$ and the ejected parton at $-\ln(2xP/m)$.

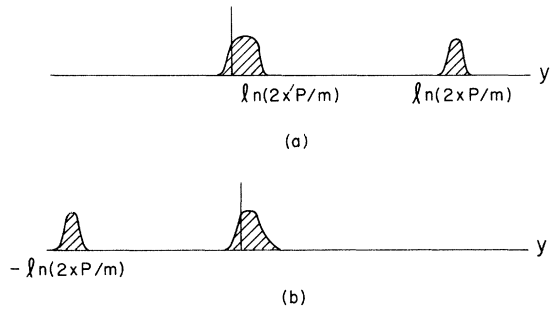

FIG. 3. (a) A parton distribution in which a single parton carries almost all the momentum of the target. (b) The parton distribution immediately after the deeply inelastic collision. Here $x \approx 1$.

unity, the about-to-be-struck parton carries almost all the target hadron's momentum. Then the parton distributions before [Fig. 3(a)] and after [Fig. 3(b)] the absorption of the virtual photon are mirror images of one another and there is an appreciable probability for elastic scattering and resonance formation. Let us develop this connection quantitatively.

According to the usual hypotheses of the parton model,[12,15] the probability that there be a gap of length Δy within a parton distribution on the rapidity axis is proportional to[12]

$$e^{-a\Delta y}, \tag{5}$$

where a is some constant. The gap between partons of longitudinal fraction x (≈ 1) and x' ($\approx 1-x$) in Fig. 3(a) is

$$\ln\left(\frac{2xP}{m}\right) - \ln\left(\frac{2x'P}{m}\right) = -\ln\left(\frac{x'}{x}\right) \approx -\ln(1-x).$$

Therefore, the probability for the gap is $(1-x)^a$. Now we need to know the range of y such that the partons near $y \approx 0$ can combine with the struck parton to form an outgoing single hadron. This range of y should include only partons which have finite momenta in this frame, i.e., "wee" partons,[12] $y \lesssim 1/P \approx 1/q_z$. So, to compute the amplitude that the struck hadron not be shattered (form factor F_1), one sums over the parton configurations with $y \lesssim 1/q_z$,

$$F_1(q) \sim \int_{1-1/q}^{1} (1-x)^a dx \sim \left(\frac{1}{q}\right)^{a+1}. \tag{6}$$

But near $x \approx 1$, νW_2 is proportional to the probability of finding a parton having longitudinal fraction x, i.e., $\nu W_2 \sim (1-x)^a$. Therefore, the threshold behavior of νW_2 is related to the falloff of the target's form factor via the same connection suggested by the resonance model.

III. HIGH-ω' ELECTROPRODUCTION AND VIRTUAL-PHOTON FRAGMENTATION

Now consider a deeply inelastic collision at large ω' (or equivalently, small $x \approx \omega'^{-1}$) as depicted in Fig. 2. Most approaches to this problem agree that the rapidity axis should be divided into (at least) three distinct kinematic regions[16]: (1) the target-fragmentation region (of length 1–2 in rapidity), (2) the central region (of length $\ln\omega'$ for large ω') between region (1) and the position of the about-to-be-struck parton, and (3) the virtual-photon (γ^*) fragmentation region (of length $\ln Q^2$) occupying the rest of the rapidity plot. It is this last region we wish to consider in some detail.

The simplest possible thing to happen after the deeply inelastic collision is that the struck parton be produced. However, it is interesting to suppose that the parton carries quark quantum numbers and that only typical hadrons are secondaries in the γ^* region. It is not self-evident that it is possible to accomplish this and preserve scaling for σ_{tot} and the other results (quantum-number sum rules, etc.) of the naive quark-parton model. One purpose of this article is to suggest that resonance models, while also predicting many features of the secondary hadrons produced in the current fragmentation region, can achieve this.

First consider an exclusive process such as γ^* +proton$\rightarrow \pi^+$ +neutron at large ω'. This is easily described in the parton model: the struck parton [at rapidity $-\ln(2xP/m)$] plus some of the wee partons of the target compose the outgoing pion, and the remaining partons compose the outgoing neutron.[17] Clearly, the physics of this process is the *same* as that reviewed in Sec. II B. Furthermore, since wee partons carry negligible momentum compared to the struck parton, the pion is produced along the virtual-photon direction. Also, since the entire γ^* region is required not to fragment, the probability for this process falls to zero quickly as Q^2 grows. In fact, it has been suggested that the cross section is[4]

$$\sigma_{\text{excl}} = \frac{1}{Q^2}(\omega')^{2\alpha-2} F_{\alpha n}{}^2(Q^2), \tag{7}$$

where $F_{\alpha n}(Q^2)$ is the transition form factor between the exchanged particle (Regge intercept α) and the produced particle n. Since the exchanged particle (Reggeon) is necessarily off its mass shell, $F_{\alpha n}$ cannot really be identified with a physical particle's form factor. However, for the case of pion exchange, the necessary extrapolation in mass is small indeed and will be ignored. Equation (7) will be applied only to this case. It is interesting that Eq. (7) is easily interpreted: The Regge term gives the probability that the quantum numbers of the exchanged particle be transferred across the

central region (length $\approx \ln\omega'$) without fragmenting, and the transition form factor gives the probability that the γ^* region (length $\approx \ln Q^2$) does not fragment. By summing Eq. (7) over n, one obtains a contribution to σ_{tot}. But what is this sum? From the resonance point of view reviewed in Sec. IIA, it is clearly the *same* sum as encountered in the discussion of the threshold behavior of νW_2. Furthermore, a sum over the secondaries in the central region must be done when computing σ_{tot}. But this region can be discussed by conventional multiperipheral methods as follows: The generalization of Eq. (7) to give the cross section for emitting m secondaries in the central region is, roughly,[18]

$$\sigma_{\{n\},m} = \frac{1}{Q^2} F_{\alpha n}{}^2(Q^2) \frac{\bar{m}^m}{m!} e^{-\bar{m}} , \tag{8}$$

where $\exp(-\bar{m})$ is the probability that the central region does not fragment. But, as explained above, $\exp(-\bar{m})$ is the Regge term $(\omega')^{2\alpha-2}$, so Eq. (8) and Eq. (7) agree when $m=0$. Summing Eq. (8) over m gives

$$\sigma_{\{n\}} \equiv \sum_m \sigma_{\{n\},m} = \frac{1}{Q^2} F_{\alpha n}{}^2(Q^2) . \tag{9}$$

Following the discussion of Sec. IIA, the remaining sum over $\{n\}$ is done as follows:

$$\begin{aligned} \sigma_{\text{tot}} &\sim \frac{1}{Q^2} \sum_n F_{\alpha n}{}^2\left(\frac{Q^2}{M_n{}^2}\right) \\ &\sim \frac{1}{Q^2} \int_{\text{const}}^{Q^2} F_\alpha{}^2\left(\frac{Q^2}{M^2}\right) \rho(M^2) dM^2 \\ &\sim \frac{1}{Q^2} \int_{\text{const}}^{Q^2} F_\alpha{}^2\left(\frac{Q^2}{M^2}\right) \frac{dM^2}{M^2} \\ &\sim \frac{1}{Q^2} \int_{\sim 1/Q^2}^{1} F^2(y^{-1}) \frac{dy}{y} \\ &\sim \frac{1}{Q^2} . \end{aligned} \tag{10}$$

So, by summing over the exclusive channels, one reproduces the scaling result for σ_{tot}. This shows, at least, an interesting consistency between our description of the threshold behavior of νW_2 and the edge of the γ^* region. It also suggests an explicit mechanism whereby the struck quark plus the quarks of the target can convert into real hadrons with probability unity. The key ingredient may be the resonant character of hadronic matter.

Continuing, one can compute the average mass-squared of the hadronic matter in the γ^* region:

$$\begin{aligned} \bar{M}^2 &\sim \sum_n M_n{}^2 F_{\alpha n}{}^2(Q^2) \\ &\sim \int M^2 F_\alpha{}^2\left(\frac{Q^2}{M^2}\right) \frac{dM^2}{M^2} , \quad \bar{M}^2 \sim Q^2 . \end{aligned} \tag{11}$$

This should be compared with the predictions of naive parton models[19] which do not account for the spectrum and resonant character of hadrons. In these models (softened field theories, for example) $\bar{M}^2 \sim$ constant, and the average multiplicity of stable "hadrons", $\bar{n}$, grows as $\ln\omega'$. The approach presented here gives $\bar{M}^2 \sim Q^2$, which strongly suggests that $\bar{n}$ grows with increasing Q^2.[4,12] The soft field theory approaches also (probably) cannot work without producing spatially isolated states of quark quantum numbers.[20]

It is amusing to note that the traditional resonance model presented in Sec. IIA can only describe the low ω' region of νW_2. For high ω' that description proves incomplete because it neglects s-channel background contributions. The treatment of this section does not suffer from this limitation because a sum has been made over secondaries emitted from the central region. Also, the parton-model motivation and Fig. 2 suggest that the resonance description of the γ^* region should be complete, i.e., background effects should not be as important as resonance effects here.

IV. PROPERTIES OF THE VIRTUAL-PHOTON FRAGMENTS

The type of process we have attempted to understand is diagrammed schematically in Fig. 4. What other properties of the γ^* region does this approach suggest? In a world of narrow-width resonances, the evolution of the excited hadronic state $\{n\}$ would, by factorization, be independent of its method of creation. Hence, to understand the character of the hadron spectrum in the γ^* region one may look at other reactions where very massive hadronic states are produced. But in a dual resonance model one can isolate an s-channel resonance contribution[21] to the amplitude for 2 hadrons $\to m$ hadrons as depicted in Fig. 5. The

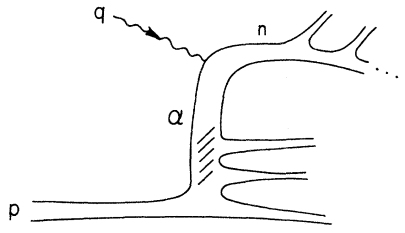

FIG. 4. A resonance-model view of the virtual-photon fragmentation region. The hadron state $\{n\}$ consists of the struck parton plus several wee partons of the target.

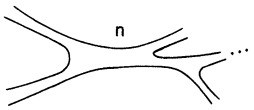

FIG. 5. An s-channel resonance contribution to the amplitude 2 hadrons $\to m$ hadrons.

states labeled $\{n\}$ here have mass $\sqrt{s}$. Furthermore, the most strongly excited states of mass $\sqrt{s}$ are peripheral, i.e., their angular momentum $\bar{l}$ is roughly $\sqrt{s}\ln s$. The peripheral character of the resonance is the crucial property governing the character of the inclusive spectrum in hadron-hadron collisions. In the dual parton model the peripheral character of the collision comes about as follows[15]: Consider the collision in the c.m. reference frame. The parton distribution in the initial state of one of the hadrons has the following properties: (1) The partons are (roughly) uniformly distributed in dx/x from $x\approx 1$ to $x\approx O(1/\sqrt{s})$; (2) only adjacent partons on the dx/x axis interact significantly; and (3) the partons random walk in the $\vec{X}$ plane transverse to the collision axis, so the mean-squared distance of a parton having longitudinal fraction x from the faster (largest x) partons is $\langle R^2(x)\rangle \sim -\ln x$. In the hadron-hadron collision only the wee partons in each wave function interact significantly,[12] so the most likely impact parameter is roughly $b(s)\sim[\langle R^2(x\approx 1/\sqrt{s}\,)\rangle]^{1/2}\sim \ln s$. Therefore, the reaction is peripheral ($\bar{l}\sim p_{\text{c.m.}}\, b(s)\sim\sqrt{s}\ln s$) as claimed. It is essential to ask now whether the resonant state ($\bar{M}^2\sim Q^2$) produced in the γ^* region is also peripheral. The parton distribution of this state (described in the reference frame of Sec. II B) consists of the struck parton plus several wee partons. According to properties (1)–(3) above, the mean-squared transverse size of this state is roughly $\langle R^2(x\sim 1/Q^2)\rangle \sim \ln Q^2$. Since the momentum of the struck parton is $\sim Q$, the most likely angular momentum of this state is $\bar{l}\sim Q\ln Q^2$. Therefore, it is very tempting to associate the states $\{n\}$ of Figs. 4 and 5, and *conjecture* that the gross dynamical features of the secondaries in the γ^* region will be the same as those of the secondaries in typical hadron-hadron collisions. Recall that the hadronic secondaries of hadron-hadron reactions

(a) Feynman scale [the single particle inclusive spectrum normalized by the total cross section becomes independent of the c.m. energy ($\frac{1}{2}\sqrt{s}$) of the reaction for large s],

(b) have bounded transverse momenta (relative to the collision axis),

(c) have logarithmic average multiplicity [$n(s)\sim\ln s$],

(d) have short-range correlations in rapidity.

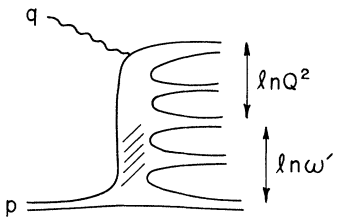

FIG. 6. The graph of Fig. 4 drawn in "multiperipheral" configuration. The γ^* region ($\ln Q^2$) and the central region ($\ln\omega'$) are labeled. Nonresonant effects are important in the central region.

These properties will now be assumed for the hadronic secondaries in the γ^* region.

Of course, an s-channel description of a production process is extremely clumsy. However, in a world of narrow resonances, Fig. 4 (now interpreted as an amplitude) can also be calculated in a multiperipheral configuration[22] as, for example, in Fig. 6. Diagrams of this topological type have been suggested on intuitive grounds within the context of the quark-parton model.[23,12] They are described in picturesque fashion as follows: The struck parton which is initially isolated in momentum space (Fig. 2) generates a cascade of partons via short-range interactions on the rapidity axis. The last partons on this cascade have low subenergy relative to some partons of the target. These partons are supposed to interact with the wee partons of the target, and the fractional charge originally carried by the struck parton is neutralized by the fractional charge of the fragments of the target. This mechanism has also suggested properties (a)–(d) listed above, but its assumption that only partons nearby in momentum space interact significantly probably leads to quark-parton production.[20] It is interesting, however, that the approach developed here makes similar predictions for the character of the final-state hadrons in deeply inelastic processes. However, the dynamical development of the struck parton into hadrons is different in the two approaches. In the present approach the struck parton interacts *directly* with some wee partons of the target. This hadronic state is extremely unstable so it breaks via the production of some parton-antiparton pairs. This mechanism repeats itself as depicted in Fig. 4 until only stable low-mass hadrons are found in the final state. The most likely decay route for a peripheral resonance has been described within the context of the dual resonance model.[24] The peripheral resonance of mass squared $\bar{M}^2$ most likely decays into a ground-state hadron plus a resonance of mass squared $\beta\bar{M}^2$ ($0\leq\beta<1$) as depicted in Fig. 7. This process repeats n times until $\beta^n\bar{M}^2\sim O(1)$ at which point the decay chain must

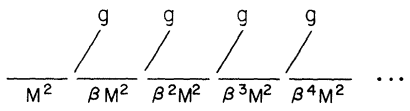

FIG. 7. The decay chain of an average (peripheral) resonance in the dual resonance model. g = ground state.

terminate, i.e., the decay process results in a multiplicity of stable low-mass hadrons $\bar{n}$ growing as $\ln\overline{M}^2$. This is the familiar logarithmic multiplicity common to most "multiperipheral" models.

Before proceeding with an illustrative calculation, we should discuss the plausibility of the remarks outlined in the previous paragraphs. First, equating states $\{n\}$ of Figs. 4 and 5 constitutes a strong assumption. Two reasons to suspect that it may be reasonable, however, are (1) the success of the Bloom-Gilman finite-energy sum rules for νW_2, and (2) the fact that nucleon resonances satisfy Elitzur's Q^2/M^2 scaling. Conventional duality ideas have had some success in describing deeply inelastic physics. A second objection might observe that the parton configuration immediately after absorbing a very virtual photon contains an immense gap. Such a configuration seldom if ever appears in purely on-shell hadronic collisions. The approach adopted here suggests that these configurations of partons are (roughly) high mass states of hadronic matter.

Clearly, one would like to have a theory which incorporates Bjorken scaling, the quark-parton model, and the mass spectrum of hadrons. Until that ambitious program is accomplished (assuming it is possible), it is interesting to make predictions from this point of view and let experiment decide if the approach is worth further development. The properties (a)–(d) above, for example, will be testable at N.A.L.

V. EDGE OF THE γ^* REGION

Consider inclusive electroproduction $\gamma^*(q)$ + hadron(p) → hadron(k) + anything in the lab frame. Suppose the produced hadron has momentum k near its kinematic maximum. Defining the longitudinal fraction $z = k_z/q_z$, kinematics reveals that for large ω',

$$1 - z \simeq \frac{M_k^2}{s} \simeq \frac{M_k^2}{\omega' Q^2}\ , \tag{12}$$

where M_k is the mass of the hadron of momentum k. When Eq. (12) is satisfied, the missing mass of the unobserved hadrons is necessarily of $O(1)$. Hence, the inclusive spectrum is composed of just a few exclusive channels,

$$\sigma_{\text{excl}}\Delta M_k^2 \sim \frac{d\sigma_{\text{incl}}}{dz}\, dz\ . \tag{13}$$

Using Eq. (7) for σ_{excl} and the Feynman scaling assumption for $d\sigma_{\text{incl}}/dz$ implies

$$\frac{1}{Q^2}(\omega')^{2\alpha-2} F_{\alpha n}^{\ 2}(\omega'^{-1}(1-z^{-1}))\, s\, dz \sim \frac{1}{Q^2} f(z) dz\ . \tag{14}$$

Suppose as before that $F_{\alpha n}$ is power-behaved for large values of its argument, $F_{\alpha n}(y) \sim y^{-n}$. Then Eq. (14) becomes

$$\begin{aligned} &\frac{1}{Q^2}(\omega')^{2\alpha-2+2n}(1-z)^{2n} s \sim \frac{1}{Q^2} f(z)\,, \\ &\frac{M_k^2}{Q^2}\left(\frac{s}{Q^2}\right)^{2\alpha-2+2n}(1-z)^{2n-1} \sim \frac{1}{Q^2} f(z)\,. \end{aligned} \tag{15}$$

The Q^2 dependences on both sides of Eq. (15) must match, so

$$n = 1 - \alpha. \tag{16}$$

Now Eq. (15) reduces to

$$\frac{M_k^2}{Q^2}(1-z)^{2n-1} \sim \frac{1}{Q^2} f(z)\,. \tag{17}$$

So, the inclusive spectrum $f(z)$ falls as $(1-z)^{2n-1}$ near the kinematic boundary. This is identical to the threshold theorem for νW_2 (target = exchanged particle). However, $n = 1 - \alpha$, so $2n - 1 = 1 - 2\alpha$ and

$$f(z) \sim (1-z)^{1-2\alpha}, \tag{18}$$

which is Feynman's boundary condition[12] familiar from purely hadronic reactions. Furthermore, the dominant transition form factor $(\alpha \to n)$ becomes

$$F_{\alpha n}(Q^2) \sim (Q^2)^{\alpha-1}\,. \tag{19}$$

So, the dominant pion transition form factors are predicted to fall as Q^{-2}.

Results of this type have recently been obtained via similar correspondence arguments.[4] The approach presented here emphasizes that an economical description of the edges of inclusive spectra (νW_2 near threshold, the edge of the γ^* region, the edge of inclusive hadron reactions, the edge of the hadron distribution produced in e^+e^- annihilation, etc.) is possible simply because the underlying physics is the same in all cases. The reader is referred to Ref. 4 for additional related results and applications.

VI. DISCUSSION

We conclude with several remarks:

(1) Our illustrations have been done for large $\omega' \gg 1$ and $\omega' \approx 1$. This is not necessary, although these limiting cases are the easiest. For $\omega' \approx 2$–12 the virtual photon strikes a parton which car-

ries a sizeable fraction of the target's (proton, say) momentum P. The quantum numbers of this parton are expected to be intimately related to the properties of the target.[12,15] The struck parton is then at the edge of the γ^* region, and it associates itself with some of the wee partons in the target and makes up an outgoing hadronic state. Since the wee parton distributions are universal (on the average their quantum numbers are independent of those of the target—an equal mixture of $\mathcal{P}$, $\mathcal{N}$, $\overline{\mathcal{P}}$, and $\overline{\mathcal{N}}$ quarks plus a small fraction of λ, $\overline{\lambda}$ pairs is often assumed), the quantum numbers of the hadrons produced at the edge of the γ^* region should reflect the internal structure of the target. In short, to study the properties of the target, do not look at its remnants—look at the remnants of the γ^*.

Within the context of simple models, one can make some striking predictions along these lines. Suppose, for example, that the struck parton was a $\mathcal{P}$ quark. It can bind with an $\overline{\mathcal{N}}$ wee parton, an $\overline{\mathcal{N}}\overline{\mathcal{P}}\mathcal{P}$ group of wee partons, $\overline{\mathcal{N}}\mathcal{N}\overline{\mathcal{N}}$ group, or $\overline{\mathcal{N}}\,\overline{\mathcal{P}}\,\mathcal{P}\overline{\mathcal{N}}\mathcal{N}$ group, etc., to form an outgoing π^+, or a ρ^+, say. Is there any reason to suppose that the simplest event (that the $\mathcal{P}$ just binds with the $\overline{\mathcal{N}}$) is the most likely? Consider the problem within the the context of simple composite models ($\lambda\varphi^3$ graphs, for example). Then we want to know the relative likelihood of the graphs drawn in Figs. 8(a), 8(b), and 8(c). These amplitudes fall as s^{-1}, s^{-2}, and s^{-3}, respectively,[25] so the simplest graph dominates. One might guess, however, that the multiple exchange graphs might Reggeize via the graphs in Fig. 8(d), and become more important than Fig 8(a). However, explicit calculations show that this does not occur and the simplest graph dominates.[20] So, within this framework, the external π^+ or ρ^+, say, would be made up of quarks according to the prescription of the low-energy quark model. It is interesting that the reason for this *low* energy prescription lies in the fact that the process occurs with a *large* subenergy.

Admittedly, the considerations of the previous paragraph are model-dependent. However, they are rather easily testable. Consider, for example, neutrino production at large ω'. The parton ejected to the edge of the γ^* region is then either a $\mathcal{P}$ or $\overline{\mathcal{N}}$ quark. Consider only events in which there is a *single* pion in the γ^* region and sum over hadronic secondaries in the central and target fragmentation regions. Since ω' is large, the missing mass of the unobserved hadronic secondaries can be chosen large (as large as $\omega' M$, for example) and, by the usual Regge-Mueller analysis,[26] should not influence the relative rates of π^+, π^-, or π^0 production near the edge of the γ^* region. So, the low-energy prescription can be applied without additional reservation and the relative rates of single π^+, π^0, and π^- production in the γ^* region should be $2:1:0$.

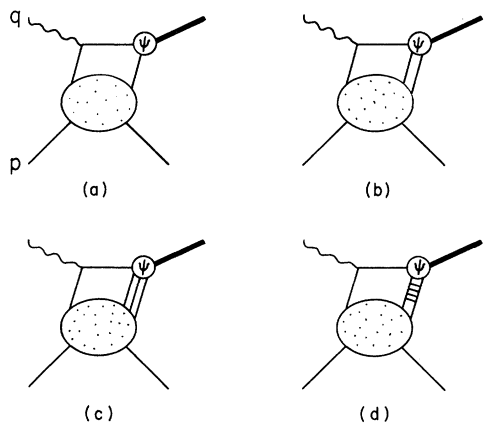

FIG. 8. Possible graphs contributing to exclusive electroproduction in a bound-state model. ψ labels the wave function of the composite state produced in the γ^* region.

Many more predictions of this type can be made. It is interesting that recent studies of the final states of electroproduction show dramatic π^+/π^- asymmetries in the γ^* region.[27] Such asymmetries are expected from the point of view developed here (given that a $\mathcal{P}$ quark is most likely struck), but a precise estimate of the asymmetry is more difficult in this case.

(2) The program discussed here is a rather speculative attempt to unify the good properties of the quark-proton model (Bjorken scaling, quantum-number considerations) with a realistic view of hadron dynamics (no asymptotic states of quark quantum numbers, resonant hadronic matter). It is, therefore, important to ask whether the usual light-cone dominance[28] and sum rules of the naive quark-parton model will remain valid in this description. The crucial property of the final state interaction which suggests this is the softness of the interaction which converts the struck parton plus several wee partons into a hadronic state. The idea is that when the struck parton interacts with some wee partons, its momentum is not changed significantly and its quantum numbers, spin, etc., are entirely unaffected. So, the calculation of forward virtual Compton scattering in the Bjorken limit should be the same *as if* there were no final state interactions. In particular, the leading light-cone singularity of the light-cone product of electromagnetic currents should be unaffected by the (crucial) interaction between the struck and wee partons. Similarly, the familiar quantum-number sum rules of the naive quark-parton model should remain valid in this approach. It would

be extremely instructive to construct a calculational parton model with the properties discussed in this paper to explicitly check this remark.

(3) The discussion of Sec. V can be carried out for exchanged particles other than pions. For example, that analysis suggests that dominant nucleon-transition form factors will fall faster with Q^2 than those for pions. Accordingly, more pions are expected near the edge of the γ^* region than nucleons. The reader is referred to Ref. 4 for more details.

(4) The same type of analysis suggested in Sec. IV for electron- and neutrino-induced reactions can be carried out for colliding beams. Here the virtual (timelike) photon dissociates into a quark-antiquark pair (Fig. 9). Each member of the pair associates with some vacuum partons (Fig. 9) and forms outgoing hadrons. The analysis of this reaction becomes very similar to that presented here. The character of the final states is similar.[29]

(5) It should be clear from Sec. V, for example, that our comments on high ω' electroproduction do not apply to diffractive production of vector states. The role of shadow scattering in resonance pic-

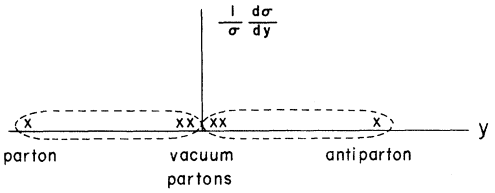

FIG. 9. The parton distribution on the rapidity axis immediately after the dissociation of the virtual (timelike) photon into a quark-antiquark pair.

(6) The remarks contained in Sec. IV of this article suggest a quark-parton picture of hadronic final states. It would be interesting to develop a *calculational* model—complete with wave functions, parton-antiparton creation processes, etc.—which embodies these suggestions. One might learn quite a lot from such an exercise.

ACKNOWLEDGMENT

The author thanks Professor J. D. Bjorken for reading a preliminary version of this article and for several encouraging suggestions. He also

man.
[22]Dual-model approaches to inclusive spectra have been considered by many authors. See, for example, C. E. DeTar, Kyungsik Kang, Chung-I Tan, and J. H. Weis, Phys. Rev. D 4, 425 (1971).
[23]S. Berman, J. D. Bjorken, and J. Kogut, Phys. Rev. D 4, 3388 (1971); Gronau, F. Ravndal, and Y. Zarmi, Nucl. Phys. B51, 611 (1973).
[24]M. B. Green and G. Veneziano, Phys. Lett. 36B, 477 (1971).
[25]These estimates are true in the approximation that the wave function ψ in Fig. 8 is replaced by point couplings. If ψ has additional structure, the exact calculations for the various graphs change, but their order in importance does not (at least for simple bound-state models). This fact is all that the argument in the text requires.
[26]A. H. Mueller, Phys. Rev. D 2, 2963 (1970).
[27]J. T. Dakin, G. J. Feldman, W. L. Lakin, F. Martin, M. L. Perl, E. W. Petraske, and W. T. Toner, Phys. Rev. Lett. 29, 746 (1972).
[28]For a recent review, see Y. Frishman, rapporteur talk presented at the XVI International Conference on High Energy Physics, Chicago-NAL, Ill. 1972 (unpublished).
[29]Relationships between the character of final states (multiplicities especially) in e^+e^- annihilation and deep-inelastic electroproduction have been noted within the context of the parton model by R. N. Cahn, J. W. Cleymans, and E. W. Colglazier, Phys. Lett. 43B, 323 (1973).

PHYSICAL REVIEW D VOLUME 8, NUMBER 9 1 NOVEMBER 1973

Duality and the Baryon Spectrum*

Richard H. Capps
Physics Department, Purdue University, West Lafayette, Indiana 47907
(Received 18 June 1973)

Various authors have found solutions to consistency equations based on duality for meson-meson and meson-baryon scattering amplitudes. It is pointed out that there are three simple solutions for the baryon spectrum and interactions that accommodate the observed lightest baryons. The differences in these solutions are discussed. Experimental data involving the third and fourth quark-model levels can be used to test which, if any, of these solutions is approximately correct.

I. INTRODUCTION

In the past several years two complimentary approaches have been used to predict the spectrum of of hadrons and hadron resonances, and their principal decay amplitudes. In the first, bootstrap conditions based on duality are applied to meson-meson and meson-baryon scattering amplitudes. In the second, a quark model is constructed in such a way as to satisfy certain consistency conditions.

Both approaches lead to the prediction of a quark-model spectrum, with hadron-hadron-hadron interactions corresponding approximately to the symmetry $SU(6)_W \otimes O(2)_{L_z}$.[1] (The symbol L denotes the total quark-model internal orbital angular momentum.) However, different solutions to the various consistency conditions differ in the baryon representations expected to exist, and in many of the baryon-baryon-meson interactions.

If the only baryons considered are those of the two lightest supermultiplets, the $(\underline{56},\underline{1})$ and $(\underline{70},\underline{3})$ of $SU(6)\otimes O(3)$, it is impossible to distinguish between some of the solutions, because the symmetry determines all the interaction ratios. Fortunately, data concerning heavier baryon resonances are beginning to accumulate now. The purpose of this paper is to show that such data can distinguish between solutions to the consistency conditions. We point out some measurements that may be crucial.

The consistency conditions and solutions are discussed in Sec. II. Although different authors have used slightly different sets of conditions, most sets have in common the same three simple solutions that fit the lightest hadrons. The experimental ways of distinguishing these three solutions are discussed in Sec. III.

II. THE DUALITY CONDITIONS AND SOLUTIONS

We consider a hadron-hadron scattering amplitude in the channel of the Mandelstam variable s, identifying the forward and backward directions as the regions of small t and u, respectively. The duality condition is that an appreciable energy region exists where both the Regge and resonance representations are valid for the imaginary part of the amplitude T. Thus,

$$\langle \mathrm{Im}T_t^{\mathrm{Regge}} \rangle = \langle \mathrm{Im}T_f^{\mathrm{res}} \rangle , \tag{1a}$$

$$\langle \mathrm{Im}T_u^{\mathrm{Regge}} \rangle = \langle \mathrm{Im}T_b^{\mathrm{res}} \rangle , \tag{1b}$$